minerals

MDPI

Article

Nb–Ta–Ti Oxides in Topaz Granites of the Geyersberg Granite Stock (Erzgebirge Mts., Germany)

Miloš René

Institute of Rock Structure and Mechanics, v.v.i., Academy of Sciences of the Czech Republic, V Holešovičkách 41, 182 09 Prague 8, Czech Republic; rene@irsm.cas.cz; Tel.: +420-266-009-228

Received: 26 November 2018; Accepted: 28 February 2019; Published: 4 March 2019

Abstract: Oxide minerals (Nb–Ta-rich rutile, columbite-group minerals and W-bearing ixiolite) represent the most common host for Nb, Ta and Ti in high-F, high-P_2O_5 Li-mica granites and related rocks from the Geyersberg granite stock in the Krušné Hory/Erzgebirge Mts. batholith. This body forms a pipe like granite stock composed of fine- to middle-grained, porphyritic to equigranular high-F, high-P_2O_5 Li-mica granites, which contain up to 6 vol. % of topaz. Intrusive breccia's on the NW margin of the granite stock are composed of mica schists and muscovite gneiss fragments enclosed in fine-grained aplitic and also topaz- and Li-mica-bearing granite. Columbite group minerals occur usually as euhedral to subhedral grains that display irregular or patched zoning. These minerals are represented by columbite-(Fe) with Mn/(Mn + Fe) ratio ranging from 0.07 to 0.15. The rare Fe-rich W-bearing ixiolite occurs as small needle-like crystals. The ixiolite is Fe-rich with relatively low Mn/(Mn + Fe) and Ta/(Ta + Nb) values (0.10–0.15 and 0.06–0.20, respectively). Owing to the high W content (19.8–34.9 wt. % WO_3, 0.11–0.20 apfu), the sum of Nb + Ta in the ixiolite does not exceed 0.43 apfu. The Ti content is 1.7–5.7 wt. % TiO_2 and Sn content is relatively low (0.3–4.1 wt. % SnO_2).

Keywords: topaz granite; Nb–Ta rutile; columbite; ixiolite; Saxothuringian Zone

1. Introduction

Niobium- and tantalum-bearing oxide minerals are common in topaz granites and related rocks (pegmatites, alkali-feldspar syenites). The most common Nb–Ta-bearing minerals in these parageneses are Nb–Ta-bearing rutile and columbite-group minerals.

In the Krušné Hory/Erzgebirge region, these minerals were described in the past by Johan and Johan [1], Rub et al. [2] and Breiter [3] from the Cínovec granite cupola, by Breiter et al. [4] from the Podlesí granite stock and by René and Škoda [5] from the Krásno-Horní Slavkov ore district in the Slavkovský Les Mts. In the German part of the Krušné Hory/Erzgebirge region, these minerals occur especially in the Sauberg, Vierung and Geyersberg granite stocks. The Sauberg and Vierung granite stocks are part of the Ehrenfriedersdorf Sn–W–Nb–Ta ore deposit. However, the Sn–W–Nb–Ta mineralisation from all of these granite stocks were only briefly described in the past, without a detailed description of the Nb–Ta mineralisation [6,7]. The Ehrenfriedersdorf ore deposit has been closed since 1990 and Nb–Ta–Ti minerals can only be sampled from various mineralogical collections. The Geyersberg granite stock lies in the most significant area of old mining subsidence ("Pinge") which has recently been opened for geological excursions. Various fractionated granites were sampled during final operations before the closing down of the Sn-W mining in this area. This author also later studied the petrology, geochemistry and mineralogy of these granites. Thus, the aim of the presented paper is a detailed description of mineralised granites, including their mineralogy and the composition of Nb-Ta-Ti minerals. The composition of Nb–Ta–Ti minerals was further correlated with distinctly better described Nb–Ta–Ti minerals from the Czech part of the Krušné Hory/Erzgebirge region [1–5].

2. Geological Setting

The Variscan granitoid rocks in the Krušné Hory/Erzgebirge and Slavkovský Les Mts. form a discontinuous belt extending about 160 km along the Czech-German border in a NE–SW direction. The belt comprises an area of about 6000 km^2 and is positioned near the southern border of the Saxothuringian zone at the northwestern edge of the Bohemian Massif (Figure 1). These granitoid rocks were successively emplaced in the Late Carboniferous and early Permian and intruded into folded and metamorphosed lithostratigraphic units consisting of Proterozoic paragneisses, late Proterozoic-Cambrian mica schists and phyllites as well as quartzites of predominantly Ordovician age [8–11].

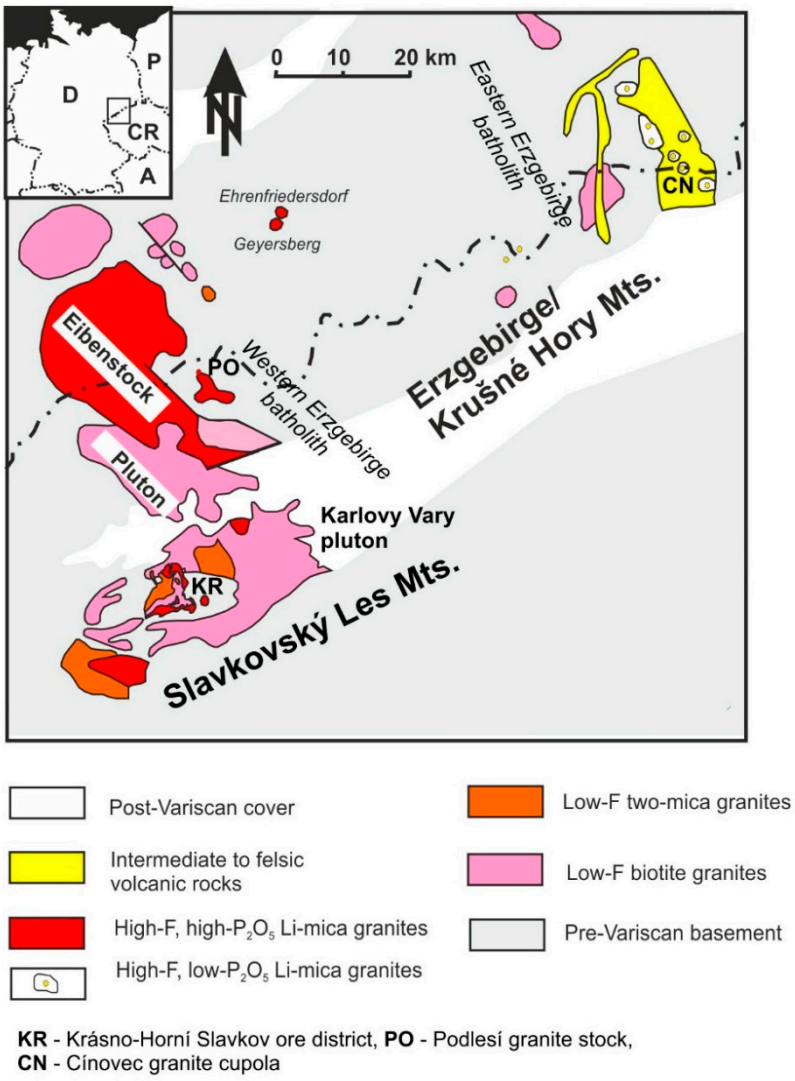

Figure 1. Geological map of the Krušné Hory/Erzgebirge batholith, modified after [9].

The Krušné Hory/Erzgebirge batholith consists of three individual plutons: Western, Middle and Eastern, each representing an assembly of shallowly emplaced granite units about 6–10 km paleodepth, with a maximum preserved vertical thickness of the pluton 10–13 km below the present surface level [12,13]. All these granites have been grouped in a number of ways in the past [14–20]. Recently, the mostly used classification of these granites subdivides them into late collisional and post-collisional granites. The late collisional granites were divided into the following three groups: (1) low-F biotite granites, (2) low-F two-mica granites and (3) high-F, high-P_2O_5 Li-mica granites.

The post-collisional granites were divided into high-F, low-P_2O_5 Li-mica granites and medium-F, low-P_2O_5 biotite granites [8,20].

The Geyersberg granite stock is one of the shallow intrusive granite bodies in the middle section of the Krušné Hory/Erzgebirge batholith. These granite bodies (Vierung, Sauberg, Geyersberg, Ziegelberg and Greifenstein) are located near the old mining towns of Ehrenfriedersdorf and Geyer. The occurrence of granite stocks and ridge-shaped apical parts of the Middle Erzgebirge granite pluton is controlled by the NW-SE striking Geyer-Elterlein-Herold shear zone, which contains the Geyer-Schönfeld, Franzenhöhe Wilischthal and Wiesenbaden fault systems. The origin of these fault systems is contemporaneous with intrusions of microgranite, aplite and lamprophyre dykes. The generation of the subsurface morphology of the above-mentioned granite stocks was investigated by numerous exploration boreholes [6,7,21] and interpreted using regional gravity measurements [22] (Figure 2).

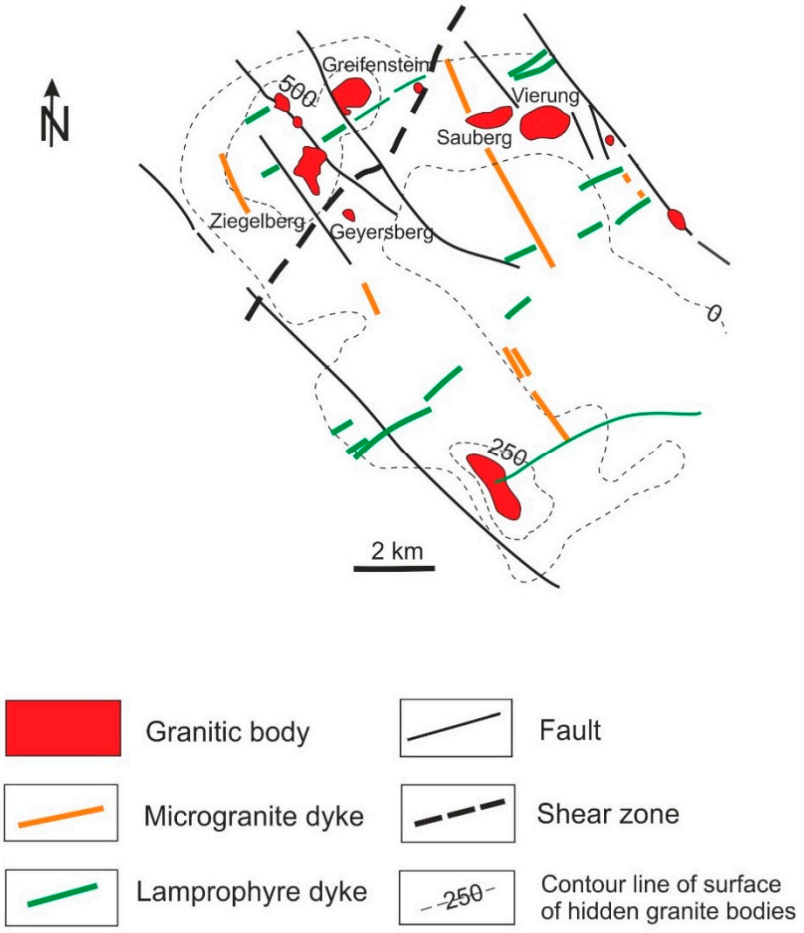

Figure 2. Geological map of the Middle part of the Krušné Hory/Erzgebirge batholith, modified after [21].

The Geyersberg granite stock forms a pipe like granite stock composed of fine- to middle-grained, porphyritic to equigranular high-F, high P_2O_5 Li mica granites, containing 2–6 vol. % of topaz. Small bodies of intrusive breccias on its NW margin are composed of mica schists and muscovite gneiss fragments enclosed in fine-grained aplitic granite. All granite varieties are partly altered (greisenisation and albitisation), mainly along steeply dipping NW-SE and NE-SW trending faults. In the western and eastern margins of the granite stock, small layers and lenses of coarse- grained marginal pegmatites (stockscheider) are present (Figure 3).

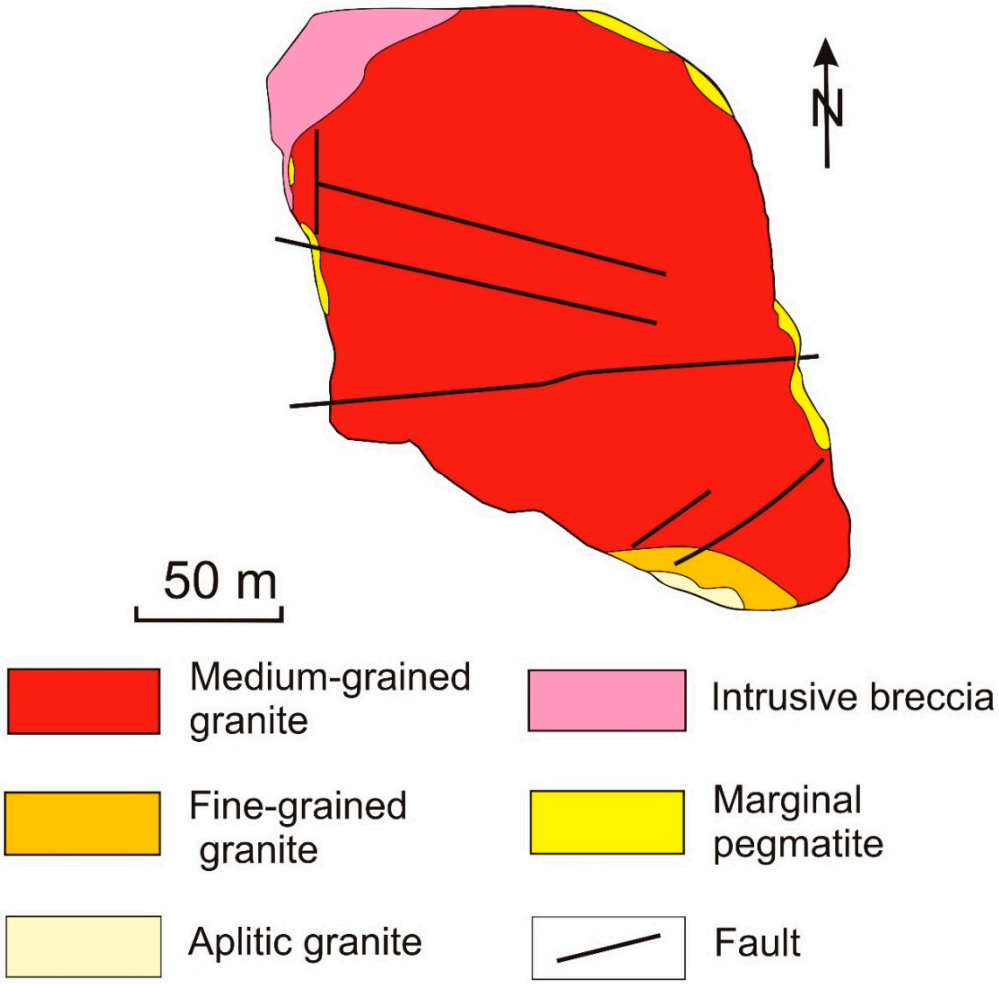

Figure 3. Geological map of the Geyersberg granite stock, modified after [7].

3. Methods

Approximately 60 quantitative electron-microprobe analyses of Nb–Ta–Ti oxides were performed using five representative samples from the Geyersberg stock. Minerals were analysed in polished thin sections to obtain information about mineral zoning in the examined rocks. Back-scattered electron images (BSE) were acquired to study the compositional variation of individual mineral grains. The abundances of Al, Bi, Ca, Fe, Mg, Mn, Nb, Sc, Si, Sn, Ta, Ti, U, W, Y and Zr were determined using a CAMECA SX 100 electron microprobe operated in a wavelength-dispersive mode at the Institute of Geological Sciences, Masaryk University in Brno, Czech Republic. The accelerating voltage and beam currents were 15 kV and 20 nA or 40 nA, respectively, with a beam diameter ranging from 1 μm to 5 μm.

The following standards were used: almandine (Al), metallic Bi (Bi), andradite (Ca, Fe, Si), olivine (Mg), spessartine (Mn), columbite (Nb), synthetic $ScVO_4$ (Sc), SnO_2 (Sn), synthetic Ta_2O_5 (Ta), TiO_2 (Ti), metallic U (U), metallic W (W), synthetic YAG (Y) and zircon (Zr). Peak count-time was 20 s and background time was 10 s for major elements, whereas for trace elements, they were 40–60 s and 20–30 s, respectively. The raw data were corrected using the PAP matrix corrections [23]. The Fe^{2+}/Fe^{3+} ratio was calculated stochiometrically.

Whole-rock composition analysis of three representative granite samples was performed (Table 1). Major elements were determined by X-ray fluorescence spectrometry using the PANalytical Axios Advanced spectrometer at Activation Laboratories Ltd., Ancaster, ON, Canada. Trace elements were determined by inductively coupled-plasma mass-spectrometry (ICP-MS) using a Perkin Elmer Sciex ELAN 6100 ICP mass spectrometer at Activation Laboratories Ltd., Ancaster, ON, Canada.

The decomposition of the rock samples for ICP-MS analysis involved lithium metaborate/tetraborate fusion. In-lab standards or certified reference materials were used for quality control. The detection limits were approximately 1–3 ppm for Ba, Rb, Sr and Zr, 0.01–0.2 ppm for Nb, Ta, Th and U and 0.002–0.05 ppm for REE. The concentration of Li_2O in analysed Li-micas was estimated using the following empirical equation: [$Li_2O = (0.289 \times SiO_2) - 9.658$], recommended by Tischendorf et al. [24].

Table 1. Chemical analyses of high-F, high-P_2O_5 Li-mica granites of the Geyersberg granite stock.

Sample	971	1543	1544
Rock-Type wt.%	**Medium-Grained Granite**	**Fine-Grained Aplitic Granite**	**Fine-Grained Aplitic Granite**
SiO_2	73.94	74.42	67.14
TiO_2	0.01	0.01	0.01
Al_2O_3	15.08	15.03	18.73
Fe_2O_3 tot.	1.04	1.28	0.90
MnO	0.03	0.03	0.03
MgO	0.10	0.04	0.05
CaO	0.59	0.51	0.60
Na_2O	4.40	3.80	5.68
K_2O	3.18	3.54	5.37
P_2O_5	0.51	0.55	0.76
L.O.I.	0.80	1.02	1.10
Total	99.68	100.23	100.37
ASI	1.28	1.37	1.15
ppm			
Ba	30.0	16.0	12.0
Rb	1190.0	1390.0	1660.0
Sr	54.0	50.0	52.0
Y	1.1	0.5	0.5
Zr	121.0	14.0	17.0
Nb	33.1	92.8	101.0
Th	5.8	5.5	13.4
Ga	62.0	75.0	96.0
Zn	71.0	185.0	98.0
Hf	4.2	2.3	3.3
Cs	41.8	41.8	28.4
Ta	37.1	68.3	76.4
U	10.8	19.5	27.1
La	1.08	0.11	0.07
Ce	2.05	0.21	0.12
Pr	0.22	0.04	0.03
Nd	0.84	0.15	0.09
Sm	0.18	0.07	0.04
Eu	0.17	0.02	0.01
Gd	0.17	0.07	0.05
Tb	0.03	0.01	0.01
Dy	0.20	0.06	0.05
Ho	0.04	0.01	0.01
Er	0.10	0.02	0.01
Tm	0.01	0.01	0.01
Yb	0.09	0.02	0.02
Lu	0.01	0.00	0.00
La_N/Yb_N	8.01	3.71	2.36
Eu/Eu *	2.99	0.70	0.55

Fe_2O_3 tot.—total Fe_2O_3, L.O.I.—loss on ignition, ASI—aluminium saturation index, La_N/Yb_N—ratio of La and Yb normalized by their concentration in chondrites, $Eu/Eu^* = Eu_N/\sqrt{[(Sm_N) \times (Gd_N)]}$, normalized by their concentrations in chondrite.

4. Results

4.1. Petrology

The main granite variety of the Geyersberg stock is formed by high-F, high-P_2O_5 Li-mica medium-grained granites composed of albite ($An_{0–1}$) (27–35 vol. %), quartz (30–34 vol. %), K-feldspar ($Or_{91–98}Ab_{2–9}An_0$) (21–30 vol. %), Li-mica (4–8 vol. %) and topaz (2–6 vol. %). Apatite, columbite-group minerals, Nb–Ta-rich rutile, zircon, cassiterite, monazite and uraninite are accessories. Apatite occurs in two generations. Older, magmatic apatite is formed by grains up to 150 μm. The younger, metasomatic apatite occurs as micro grains (1–2 μm) enclosed in partly albitised plagioclases. The partly altered albite also contains many micro grains of apatite. Both feldspars are enriched in P (up to 0.8 wt. % P_2O_5). Lithian mica, according to the classification of Tischendorf et al. [24], is represented by Fe-rich polylithionite. Estimated lithium contents in analysed lithian micas reach up to 2.7 wt. % Li_2O.

The fine-grained aplitic granite, which also includes the intrusive breccias, contains quartz (32–33 vol. %), albite ($An_{0–1}$) (29–32 vol. %), K-feldspar ($Or_{94–98}Ab_{2–6}An_0$) (28–30 vol. %), Li-mica (2–4 vol. %) and topaz (2 vol. %). Accessories are apatite, Nb–Ta-rich rutile, columbite-group minerals, cassiterite, zircon, ixiolite and, rarely, uraninite. The K-feldspar is sometimes enriched in P (up to 1. 2 wt. % P_2O_5). Apatite occurs in two generations: older, magmatic apatite is formed by grains up to 100 μm big. The younger, metasomatic apatite occurs as micro grains (1–2 μm) enclosed in partly albitised plagioclases. Lithian mica is represented by Fe-rich polylithionite with estimated lithium contents up to 2.8 wt. % Li_2O.

4.2. Geochemistry

The medium grained high-F, high-P_2O_5 Li-mica granite of the Geyersberg stock is a peraluminous S-type granite with an aluminium saturation index from 1.2 to 1.5. In comparison with common S-type granites [25], it is enriched in incompatible elements, such as Rb (1190 ppm), Cs (42 ppm), Sn (229 ppm), Nb (33 ppm), Ta (37 ppm) and W (11 ppm), however is poor in Mg (0.05 wt. %), Ca (0.6 wt. %), Sr (54 ppm), Ba (30 ppm) and Zr (121 ppm). The fine-grained aplitic granite is also enriched in incompatible elements like Rb (1390–1660 ppm), Cs (28–42 ppm), Nb (93–101 ppm) and Ta (68–76 ppm), however is poor in Mg (0.04–0.05 wt. % MgO), Ca (0.5–0.6 wt. % CaO), Sr (50–52 ppm), Ba (12–16 ppm) and Zr (14–17 ppm) (Table 1).

4.3. Mineralogy of the Ti–Nb–Ta Oxide Assemblage

4.3.1. Nb–Ta-Rich Rutile

Rutile is the most common Nb and Ta carrier in fine-grained aplitic granite. Rutile occurs mostly as inclusions in lithium mica flakes where it forms subhedral crystals. The majority of examined grains display irregular zoning (Figure 4). These grains contain very low concentrations of Nb (0.3–4.5 wt. % Nb_2O_5) and Ta (0.02–1.1 wt. % Ta_2O_5). Also present are Sn and W (0.6–2.4 wt. % SnO_2, 0.1–3.6 wt. % WO_3). The examined rutiles have a variable Fe content (0.4–2.1 wt. % FeO), however very low Mn concentrations (0.01–0.03 wt. % MnO) (Table 2).

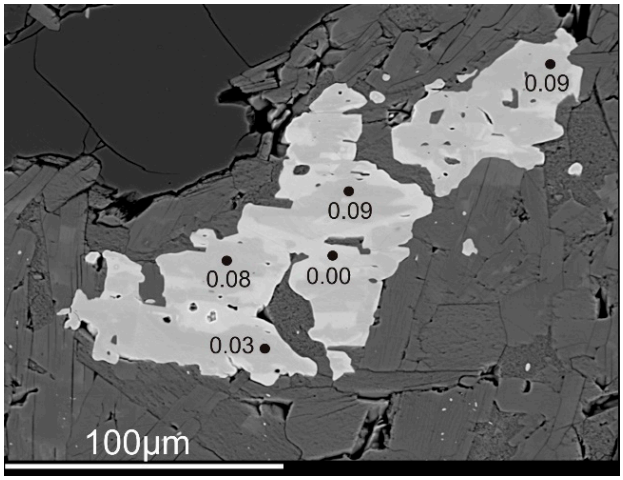

Figure 4. BSE image of zoned Nb–Ta-rich rutile showing variation in Ta/(Ta + Nb) ratio.

Table 2. Representative microprobe analyses of Nb-Ta-bearing rutile (wt. %).

Sample	1544-4	1544-5	1544-6	1544-7	1544-8	1544-12	1544-13	1544-14
WO_3	0.21	0.18	1.53	0.15	0.11	3.62	0.14	1.28
Ta_2O_5	0.05	0.05	b.d.l.	0.02	0.04	b.d.l.	0.05	0.03
Nb_2O_5	0.31	0.33	0.42	0.39	0.25	0.33	0.54	0.39
TiO_2	97.38	96.75	92.83	97.83	97.57	91.52	97.56	95.89
SiO_2	0.03	0.03	0.02	0.05	0.03	0.04	0.03	0.06
ZrO_2	b.d.l.	0.00	0.06	b.d.l.	0.01	0.07	b.d.l.	0.02
SnO_2	1.19	1.39	3.31	1.22	1.10	1.81	0.58	1.66
Al_2O_3	0.06	0.08	0.10	0.07	0.06	0.15	0.08	0.09
Fe_2O_3	0.00	0.00	0.00	0.00	0.00	0.00	0.00	0.00
FeO	0.52	0.50	0.98	0.47	0.46	1.77	0.62	0.79
MnO	0.01	0.00	0.01	0.02	0.00	b.d.l.	0.01	0.01
CaO	0.01	0.01	b.d.l.	b.d.l.	0.00	0.01	0.02	0.01
Total	99.77	99.32	99.26	100.20	99.63	99.32	99.63	100.23
				O = 2, apfu				
W^{6+}	0.00	0.00	0.01	0.00	0.00	0.01	0.00	0.00
Ta^{5+}	0.00	0.00	0.00	0.00	0.00	0.00	0.00	0.00
Nb^{5+}	0.00	0.00	0.00	0.00	0.00	0.00	0.00	0.00
Ti^{4+}	0.98	0.98	0.96	0.98	0.99	0.95	0.98	0.97
Si^{4+}	0.00	0.00	0.00	0.00	0.00	0.00	0.00	0.00
Zr^{4+}	0.00	0.00	0.00	0.00	0.00	0.00	0.00	0.00
Sn^{4+}	0.01	0.01	0.02	0.01	0.01	0.01	0.00	0.01
Al^{3+}	0.00	0.00	0.00	0.00	0.00	0.00	0.00	0.00
Fe^{3+}	0.00	0.00	0.00	0.00	0.00	0.00	0.00	0.00
Fe^{2+}	0.01	0.01	0.01	0.01	0.01	0.02	0.01	0.01
Mn^{2+}	0.00	0.00	0.00	0.00	0.00	0.00	0.00	0.00
Ca^{2+}	0.00	0.00	0.00	0.00	0.00	0.00	0.00	0.00
Total	1.00	1.00	1.00	1.00	1.01	0.99	0.99	0.99
Mn/(Mn + Fe)	0.02	0.00	0.01	0.04	0.00	0.00	0.02	0.01
Ta/(Ta + Nb)	0.09	0.08	0.00	0.03	0.09	0.00	0.05	0.04

b.d.l.—below detection limit, apfu—atoms per formula unit, O = 2.

4.3.2. Columbite-Group Minerals

Columbite-group minerals occur in both varieties of high-F, high-P_2O_5 Li-mica granites, mostly as euhedral to subhedral grains. Some grains display irregular or patched zoning (Figure 5). No systematic core-rim compositional evolution was observed. The columbite-group minerals are represented predominantly by columbite-(Fe) with a Mn/(Mn + Fe) ratio varying from 0.07 to 0.15 and with relatively low Ta/(Ta + Nb) values (0.06–0.41) (Table 3).

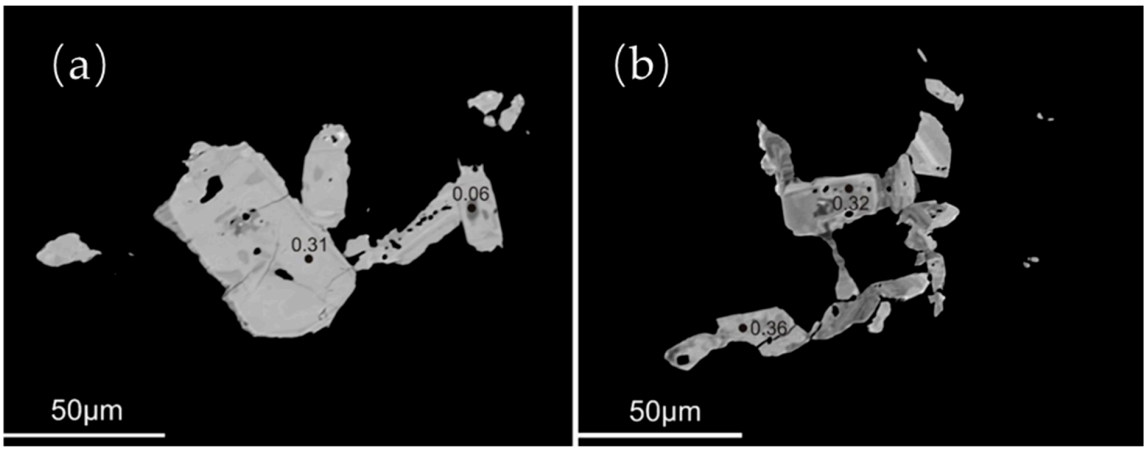

Figure 5. BSE (back-scattered electron) images of zoned columbite-(Fe) showing variation in Ta/(Ta + Nb) ratio. (**a**) The bigger grain of columbite-(Fe); (**b**) The aggregates of small zoned columbite-(Fe) grains.

Table 3. Representative microprobe analyses of columbite-group minerals (wt. %).

Sample	971-6	971-11	971-14	1543-44	1543-45	1543-47	1543-48
WO_3	2.24	2.17	1.60	4.52	2.10	3.88	5.41
Ta_2O_5	28.36	25.92	32.70	33.68	20.16	24.20	19.31
Nb_2O_5	47.79	45.73	43.41	40.66	52.96	47.10	49.45
TiO_2	2.22	4.57	2.26	2.26	4.31	4.93	4.84
SiO_2	0.00	0.02	0.00	0.02	0.05	0.04	0.03
ZrO_2	0.07	0.38	0.15	0.29	0.64	0.23	0.20
SnO_2	0.28	1.29	0.50	1.15	0.99	1.66	1.39
Al_2O_3	0.01	0.03	0.02	0.00	0.00	0.00	0.03
Y_2O_3	0.10	0.19	0.17	0.12	0.07	0.05	0.11
Sc_2O_3	0.19	0.29	0.39	0.02	0.15	0.08	0.07
Fe_2O_3	0.29	1.29	0.98	0.49	1.18	0.42	0.83
FeO	16.57	16.12	15.07	15.62	15.42	15.78	16.17
MnO	1.40	1.56	2.02	1.80	1.93	1.61	1.66
CaO	0.01	0.01	0.00	0.00	0.00	0.10	0.00
Total	99.53	99.57	99.27	100.63	99.96	100.08	99.50
			O = 6, apfu				
W^{6+}	0.04	0.04	0.03	0.08	0.03	0.06	0.09
Ta^{5+}	0.49	0.44	0.58	0.60	0.33	0.41	0.32
Nb^{5+}	1.37	1.30	1.27	1.20	1.45	1.32	1.37
Ti^{4+}	0.11	0.22	0.11	0.11	0.20	0.23	0.22
Si^{4+}	0.00	0.00	0.00	0.00	0.00	0.00	0.00
Zr^{4+}	0.00	0.01	0.01	0.01	0.02	0.01	0.01
Sn^{4+}	0.01	0.03	0.01	0.03	0.02	0.04	0.03
Al^{3+}	0.00	0.00	0.00	0.00	0.00	0.00	0.00
Y^{3+}	0.00	0.01	0.01	0.00	0.00	0.00	0.00
Sc^{3+}	0.01	0.02	0.02	0.00	0.01	0.00	0.00
Fe^{3+}	0.01	0.06	0.05	0.02	0.05	0.02	0.04
Fe^{2+}	0.88	0.79	0.82	0.85	0.78	0.82	0.83
Mn^{2+}	0.08	0.08	0.11	0.10	0.10	0.08	0.09
Ca^{2+}	0.00	0.00	0.00	0.00	0.00	0.01	0.00
Total	3.00	3.00	3.00	3.00	3.00	3.00	3.00
Mn/(Mn + Fe)	0.08	0.10	0.12	0.11	0.11	0.09	0.09
Ta/(Ta + Nb)	0.26	0.25	0.31	0.33	0.19	0.24	0.19

4.3.3. Ixiolite

In this paper, the term ixiolite is used to describe minerals of columbite-like chemical composition and W content greater than 0.10 apfu (O = 2). However, structural data confirming the identity of this

mineral are not available. The W-bearing ixiolite was observed as needle-like subhedral crystals occurring in fine-grained aplitic granite from intrusive breccias (Figure 6). The ixiolite is Fe-rich with relatively low Mn/(Mn + Fe) and Ta/(Ta + Nb) values (0.10–0.15 and 0.06–0.20, respectively). Owing to the high W content (19.8–34.9 wt. % WO_3, 0.11–0.20 apfu), the sum of Nb + Ta in the ixiolite does not exceed 0.43 apfu. The Ti content is 1.7–5.7 wt. % TiO_2 and Sn content is relatively low (0.3–4.1 wt. % SnO_2) (Table 4).

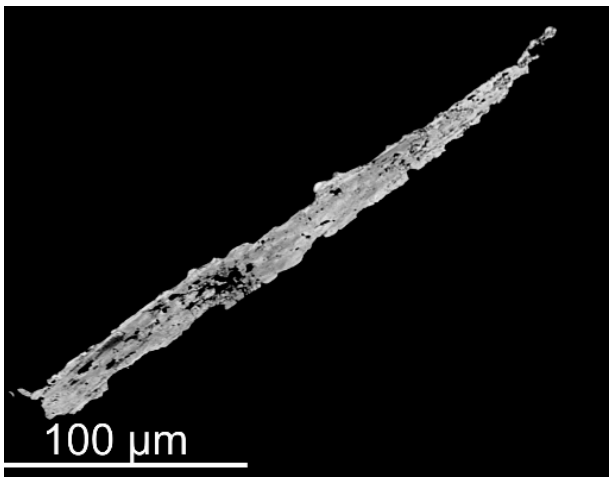

Figure 6. BSE image of W-bearing ixiolite.

Table 4. Representative microprobe analyses of ixiolite (wt. %).

Sample	1705-16	1705-19	1705-20	1705-28	1706-54
WO_3	34.89	29.20	32.06	23.76	19.81
Ta_2O_5	3.44	3.79	4.86	4.72	14.28
Nb_2O_5	31.24	37.70	31.31	42.13	34.37
TiO_2	1.69	2.03	1.72	2.35	5.68
SiO_2	0.16	0.24	0.18	0.11	0.02
ZrO_2	0.59	0.64	0.56	0.64	0.84
SnO_2	0.33	0.33	0.35	0.32	4.13
UO_2	0.05	0.05	b.d.l.	0.07	b.d.l.
Al_2O_3	0.32	0.47	0.25	0.13	0.01
Y_2O_3	b.d.l.	b.d.l.	b.d.l.	b.d.l.	0.01
Sc_2O_3	0.09	0.10	0.08	0.10	0.31
Bi_2O_3	0.33	0.49	0.28	0.32	0.06
Fe_2O_3	3.26	3.07	3.24	2.51	0.97
FeO	15.28	15.36	15.35	15.69	16.40
MnO	2.88	2.91	2.99	3.09	1.84
MgO	0.04	0.07	0.02	0.04	b.d.l.
CaO	0.18	0.21	0.08	0.06	b.d.l.
Total	94.77	96.66	93.33	96.04	98.73
		O = 2, apfu			
W^{6+}	0.20	0.16	0.19	0.13	0.11
Ta^{5+}	0.02	0.02	0.03	0.03	0.08
Nb^{5+}	0.32	0.37	0.32	0.41	0.33
Ti^{4+}	0.03	0.03	0.03	0.04	0.09
Si^{4+}	0.00	0.01	0.00	0.00	0.00
Zr^{4+}	0.01	0.01	0.01	0.01	0.01
U^{4+}	0.00	0.00	0.00	0.00	0.00
Al^{3+}	0.01	0.01	0.01	0.00	0.00
Y^{3+}	0.00	0.00	0.00	0.00	0.00
Sc^{3+}	0.00	0.00	0.00	0.00	0.01
Bi^{3+}	0.00	0.00	0.00	0.00	0.00

Table 4. *Cont.*

Sample	1705-16	1705-19	1705-20	1705-28	1706-54
Fe^{3+}	0.07	0.06	0.07	0.05	0.02
Fe^{2+}	0.34	0.33	0.35	0.32	0.31
Mn^{2+}	0.06	0.05	0.06	0.06	0.03
Mg^{2+}	0.00	0.00	0.00	0.00	0.00
Ca^{2+}	0.00	0.01	0.00	0.00	0.00
Total					
Mn/(Mn + Fe)	0.14	0.14	0.14	0.15	0.10
Ta/(Ta + Nb)	0.06	0.06	0.09	0.06	0.20

b.d.l.—below detection limit.

5. Discussion

The high-F, high-P_2O_5 Li-mica granites of the Geyersberg granite stock are very similar to the same granite varieties found in the Podlesí granite stocks or in the area of the Krásno–Horní Slavkov ore deposit [4,5] in the Czech part of the Erzgebirge/Krušné Hory region. All these granites represent highly fractionated peraluminous granitic rocks which contain variable contents of topaz and lithium micas.

Niobium and tantalum display similar geochemical behaviour during fractionation in granitic melts. During these processes, the elements are typically incompatible and may thus reach higher concentrations in highly fractionated granitic rocks. The magmatic fractionation leads to an enrichment of Ta relative to Nb and to significant decreases of the Nb/Ta ratio in these rocks [26–28]. The subsequent fractionation of Nb and Ta and decrease of the Nb/Ta ratio is coupled with subsequent hydrothermal alteration (muscovitization, greisenisation) of granitic rocks. Peraluminous granitic rocks that show significant interaction with hydrothermal fluids systematically display Nb/Ta ratios <5. Therefore, the ratio Nb/Ta = 5 appears to be a good marker to discriminate mineralized from barren peraluminous granites [29] (Figure 7). Enrichment of Ta and consequently low whole-rock Nb/Ta values were previously found in highly peraluminous granites from the Beauvoir stock in France [30,31], the Yichun complex in China [32] and the Limu complex in China [33]. In comparison with these localities, the high-F, high-P_2O_5 Li-mica granites from the Geyersberg, Krásno-Horní Slavkov ore district [5] and this study, Podlesí [34] and the high-F, low P_2O_5 Li-mica granites of the Cínovec granite cupola [2,35] of the eastern Krušné Hory/Erzgebirge batholith show a lower degree of granite fractionation and, consequently, a higher Nb/Ta ratio. The Nb enrichment of these granites probably reflects a slightly different nature of the protolith [36].

Columbite group minerals together with Nb-Ta-rich rutile are important accessory minerals in highly fractionated granitic rocks. The presence of Nb and Ta in rutile is commonly interpreted to indicate a solid solution between TiO_2 and $(Fe, Mn)(Nb, Ta)_2O_6$ [37]. The solubility of rutile in magmas varies significantly with the nature of the melt. However, its solubility in peraluminous granites is very low [38,39].

In all of these highly fractionated granites, Nb and Ta are predominantly hosted in Nb-Ta-rich rutile and, to a lesser extent, in columbite-group minerals [1–5,40] (Figure 8). The columbite-group minerals from the Geyersberg and Podlesí [4] granite stocks display relatively low Mn/(Mn + Fe) ratios, ranging from 0.07 to 0.2. The columbite-group minerals from the Krásno-Horní Slavkov district [5] and the Cínovec granite cupola [1–3] have a highly variable Mn/(Mn + Fe) ratio, ranging from 0.15 to 0.9. A similarly wide variation was observed in highly fractionated granites from Cornwall, UK and Beauvoir in France [40,41]. The highest Mn/(Mn + Fe) ratio in published literature was found in columbite-group minerals from the Yichun granite stock [32]. The increase of the Mn/(Mn + Fe) ratio in columbite-group minerals has been attributed to fractional crystallisation in mineralised granites [40,42]. Experiments showed that the solubility of columbite-(Mn) is strongly controlled by the aluminium saturation index (ASI) as well as Li and P concentrations [43,44].

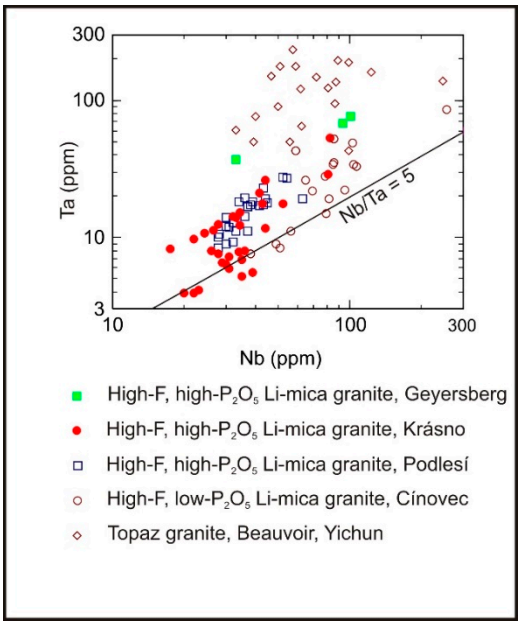

Figure 7. Ta versus Nb concentrations in high-F, high-P_2O_5 Li-mica granites and related rocks.

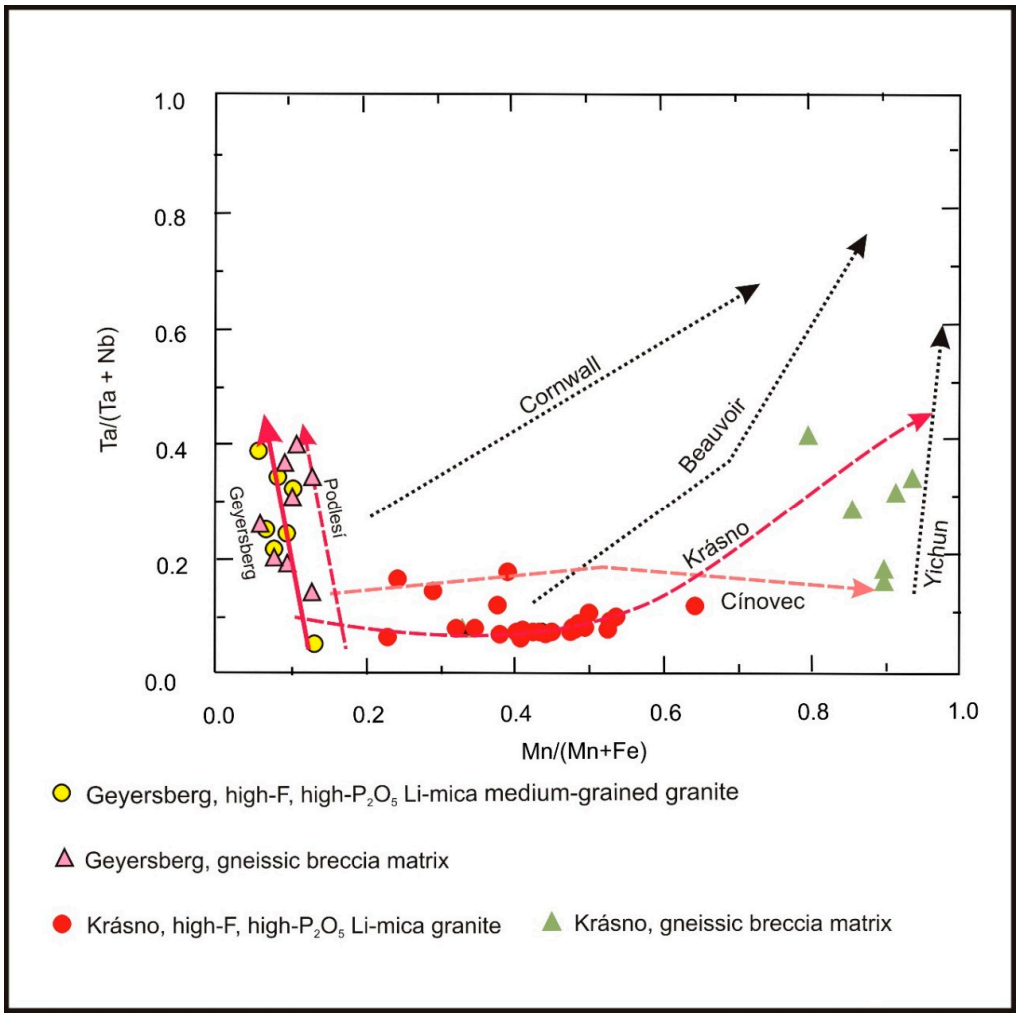

Figure 8. Schematic Ta/(Ta + Nb) versus Mn/(Mn + Fe) composition plot for columbite-group minerals from high-F, high-P_2O_5 Li mica granites and related rocks.

The W-bearing ixiolite was found as a scarce mineral phase in fine-grained aplitic granites, which occur as a matrix for intrusive breccias. The ixiolite displays low Mn/(Mn + Fe) ratios (0.10–0.15). Similar ixiolite was also found as a relatively scarce mineral phase in high-F granites from the Hub stock in the Krásno-Horní Slavkov ore district [5], Podlesí granite stock [4] and Cínovec granite cupola [1,3]. However, ixiolite from the Hub and Podlesí granite stock and from the Cínovec granite cupola displays higher Mn/(Mn + Fe) ratios (0.14–0.37). The Ta/(Nb + Ta) ratio in ixiolite from the Geyersberg stock is relatively low (0.06–0.20), whereas the Ta//(Nb + Ta) ratio in ixiolite from the Podlesí granite stock and the Cínovec cupola are higher (0.14–0.50).

6. Conclusions

The high-F, high-P_2O_5 Li-mica granites found in the Geyersberg stock are highly fractionated S-type granitic rocks (ASI = 1.2–1.5) with low Nb/Ta ratio (0.9–1.3) which contain Nb–Ta rutile and columbite-group minerals as relatively rare accessories. These Nb–Ta accessories, together with W-bearing ixiolite, represent the most significant accessory minerals. The low Nb/Ta ratio in these rocks is coupled with their hydrothermal alteration, which is characterised mainly by albitisation of plagioclase and occurrence of a younger generation of apatite. Columbite-group minerals are represented by columbite-(Fe) with Mn/(Mn + Fe) ratio ranging from 0.07 to 0.15. The rare Fe-rich W-bearing ixiolite occurs as small needle-like crystals. The ixiolite is Fe-rich with relatively low Mn/(Mn + Fe) and Ta/(Ta + Nb) values (0.10–0.15) and (0.06–0.20), respectively.

Funding: The research for this paper was carried out thanks to the support of the long-term conceptual development research organisation RVO 67985891.

Acknowledgments: Petr Gadas and Radek Škoda from the Masaryk University, Brno are thanked for their assistance during the microprobe work. I am grateful to three anonymous reviewers for numerous helpful comments and recommendations that helped to improve this paper. I wish also to thank Annika Szameitat for her English corrections.

Conflicts of Interest: The author declares no conflict of interest.

References

1. Johan, Z.; Johan, V. Accessory minerals of the Cínovec (Zinnwald) granite cupola, Czech Republic. Part 1: Nb-, Ta- and Ti-bearing oxides. *Miner. Pet.* **1994**, *83*, 113–150. [CrossRef]
2. Rub, A.K.; Štemprok, M.; Rub, M.G. Tantalum mineralisation in the apical part of the Cínovec (Zinnwald) granite stock. *Miner. Pet.* **1998**, *63*, 199–222. [CrossRef]
3. Breiter, K.; Korbelová, Z.; Chládek, Š.; Uher, P.; Knésl, I.; Rambousek, P.; Honig, S.; Šešulka, V. Diversity of Ti-Sn-W-Nb-Ta oxide minerals in the classic granite related magmatic-hydrothermal Cínovec/Zinnwald Sn-W-Li deposit (Czech Republic). *Eur. J. Miner.* **2017**, *29*, 727–738. [CrossRef]
4. Breiter, K.; Škoda, R.; Uher, P. Nb-Ta-Ti-W-Sn-oxide minerals as indicators of a peraluminous P- and F-rich granitic system evolution: Podlesí, Czech Republic. *Miner. Pet.* **2007**, *91*, 225–248. [CrossRef]
5. René, M.; Škoda, R. Nb-Ta-Ti oxides fractionation in rare-metal granites: Krásno-Horní Slavkov ore district, Czech Republic. *Mineral. Petrol.* **2011**, *103*, 37–48. [CrossRef]
6. Hösel, G.; Hoth, K.; Jung, D.; Leonhardt, D.; Mann, M.; Meyer, H.; Tägl, U. Das Zinnerz-Lagerstättengebiet Ehrenfriedersdorf/Erzgebirge. *Bergbau Sachs.* **1994**, *1*, 1–196.
7. Hösel, G.; Fritsch, E.; Josiger, U.; Wolf, P. Das Lagerstättengebiet Geyer. *Bergbau Sachs.* **1996**, *4*, 1–112.
8. Förster, H.J.; Tischendorf, G.; Trumbull, R.B.; Gottesmann, B. Late-collisional granites in the Variscan Erzgebirge (Germany). *J. Pet.* **1999**, *40*, 1613–1645. [CrossRef]
9. Breiter, K.; Förster, H.-J.; Seltmann, R. Variscan silicic magmatism and related tin-tungsten mineralization in the Erzgebirge-Slavkovský les metalogenic province. *Mineral. Depos.* **1999**, *34*, 505–521. [CrossRef]
10. Romer, R.L.; Thomas, R.; Stein, H.J.; Rhede, D. Dating multiply over printed Sn-mineralized granites—Examples from the Erzgebirge, Germany. *Miner. Depos.* **2007**, *42*, 337–359. [CrossRef]
11. Tichomirova, M.; Leonhardt, D. New age determinations (Pb-Pb zircon evaporation, Rb/Sr) on the granites from Aue-Scharzenberg and Eibenstock, Western Erzgebirge, Germany. *Z. Geol. Wiss.* **2010**, *38*, 99–123.

12. Hofmann, Y.; Jahr, T.; Jentzch, G. Three-dimensional gravimetric modelling to detect deep structure of the region Vogtland/NW Bohemia. *J. Geodyn.* **2003**, *35*, 209–220. [CrossRef]
13. Blecha, V.; Štemprok, M. Petrochemical and geochemical characteristics of late Variscan granites in the Karlovy Vary Massif (Czech Republic)—Implications for gravity and magnetic interpretation at shallow depths. *J. Geosci.* **2012**, *57*, 65–85. [CrossRef]
14. Fiala, F. Granitoids of the Slavkovský (Císařský) les Mountains. *Sbor. Geol. Věd G* **1968**, *14*, 93–160.
15. Tischendorf, G. Zur geochemischen Spezialisierung der Granite des westerzgebirgischen Teilplutons. *Geologie* **1970**, *19*, 25–40.
16. Lange, H.; Tischendorf, G.; Pälchen, W.; Klemm, I.; Ossenkopf, W. Zur petrographie und geochemie der Granite des Erzgebirges. *Geologie* **1972**, *21*, 457–492.
17. Kaemmel, T.; Just, G. Geochemical differentiation of granitoids in the G.D.R. using normalized trace element differences. *Gerlands Beitr. Geophys.* **1985**, *94*, 351–369.
18. Štemprok, M. Petrology and geochemistry of the Czechoslovak part of the Krušné hory Mts. *Sbor Geol. VědLg* **1986**, *27*, 111–156.
19. Tischendorf, G.; Geisler, M.; Gerstenberger, H.; Budzinski, H.; Vogler, P. Geochemistry of Variscan granites of the Westerzgebirge Vogtland region—An example of tin deposit-generating granites. *Chem. Erde* **1987**, *46*, 213–235.
20. Förster, H.J.; Römer, R.L. Carboniferous Magmatism. In *Pre-Mesozoic Geology of Saxo-Thuringia—From the Cadomian Active Margin to the Varisan Orogen*; Linnemann, U., Romer, R.L., Eds.; Schweizerbart: Stuttgart, Germany, 2010; pp. 287–308.
21. Hoth, K.; Ossenkopf, W.; Hösel, G.; Zernke, B.; Eisenschmidt, K.; Kühne, R. Die granite im Westteil des Mittelerzgebirgischen Teilplutons und ihr rahmen. *Geoprofil* **1991**, *3*, 3–13.
22. Tischendorf, G.; Wasternack, J.; Bolduan, H.; Bein, E. Zur Lage der granitoberfläche im Erzgebirge und Vogtland mit bemerkungen über ihre bedeutung für die verteilung endogener lagerstätten. *Z. Angew. Geol.* **1965**, *11*, 410–423.
23. Pouchou, J.L.; Pichoir, F. "PAP" (φ-ϱ-Z) Procedure for Improved Quantitative Microanalysis. In *Microbeam Analysis*; Armstrong, J.T., Ed.; San Francisco Press: San Francisco, CA, USA, 1985; pp. 104–106.
24. Tischendorf, G.; Rieder, M.; Förster, H.-J.; Gottesmann, B.; Guidotti, C.V. A new graphical presentation and subdivision of potassium micas. *Min. Mag.* **2004**, *68*, 649–667. [CrossRef]
25. Chappell, B.W.; Hine, R. The Cornubian batholith: An example of magmatic fractionation on a crustal scale. *Res. Geol.* **2006**, *56*, 203–244. [CrossRef]
26. Green, T.H. Significance of Nb/Ta as an indicator of geochemical processes in the crust-mantle system. *Chem. Geol.* **1995**, *120*, 347–359. [CrossRef]
27. Linnen, R.L.; Keppler, H. Columbite solubility in granitic melts: Consequences for the enrichment and fractionation of Nb and Ta in the Earth´s crust. *Contrib. Mineral. Petrol.* **1997**, *128*, 213–227. [CrossRef]
28. Dostál, J.; Chatterjee, A.K. Contrasting behaviour of Nb/Ta and Zr/Hf ratios in a peraluminous granitic pluton (Nova Scotia, Canada). *Chem. Geol.* **2000**, *163*, 207–218. [CrossRef]
29. Ballouard, C.; Poujol, M.; Boulvais, P.; Branquet, Y.; Tartèse, R.; Vigneresse, J.L. Nb-Ta fractionation in peraluminous granites: A marker of the magmatic-hydrothermal transition. *Geology* **2016**, *44*, 231–234. [CrossRef]
30. Raimbault, L.; Cuney, M.; Azencott, C.; Duthou, J.L.; Joron, J.L. Geochemical evidence for a multistage genesis of Ta-Sn-Li mineralization in the granite at Beauvoir, French Massif Central. *Econ. Geol.* **1995**, *90*, 548–576. [CrossRef]
31. Breiter, K.; Škoda, R. Vertical zonality of fractionated granite plutons reflected in zircon chemistry: The Cínovec A-type versus the Beauvoir S-type suite. *Geol. Carpath.* **2012**, *63*, 383–398. [CrossRef]
32. Huang, X.L.; Wang, R.C.; Chen, X.M.; Hu, H.; Liu, C.S. Vertical variations in the mineralogy of the Yichun topaz-lepidolite granite, Jiangxi province, South Chiuna. *Can. Min.* **2002**, *40*, 1047–1068. [CrossRef]
33. Zhu, J. Ch.; Li, R.K.; Li, F. Ch.; Xiong, X.L.; Zhou, F.Y.; Huang, X.L. Topaz-albite granites and rare-metal mineralization in the Limu district, Guangxi province, southeast China. *Miner. Depos.* **2001**, *36*, 393–405. [CrossRef]
34. Breiter, K. From explosive breccia to inidirectional solidification textures: Magmatic evolution of a phosphorus- and fluorine-rich granite system (Podlesí, Krušné hory Mts., Czech Republic). *Bull. Czech. Geol. Surv.* **2002**, *77*, 67–72.

35. Breiter, K.; Ďurišová, J.; Hrstka, T.; Korbelová, Z.; Hložková Vaňková, M.; Vašinová Galiová, M.; Rambousek, P.; Knésl, I.; Dobeš, P.; et al. Assessment of magmatic vs. metasomatic processes in rare-metal granites: A case study of the Cínovec/Zinnwald Sn-W-Li deposit, Central Europe. *Lithos* **2017**, *292–293*, 198–217. [CrossRef]
36. Breiter, K. Nearly contemporaneous evolution of the A- and S-type fractionated granites in the Krušné hory/Erzgebirge Mts., Central Europe. *Lithos* **2012**, *151*, 105–121. [CrossRef]
37. Černý, P.; Ercit, T.S. Some recent advances in the mineralogy and geochemistry of Nb and Ta in rare-element granitic pegmatites. *Bull. Minéral.* **1985**, *108*, 499–532.
38. Ryerson, F.J.; Watson, E.B. Rutile saturation in magmas: Implications for Ti-Nb-Ta depletion in island-arc basalts. *Earth Planet. Sci. Lett.* **1987**, *86*, 225–239. [CrossRef]
39. Keppler, H. Influence of fluorine on the enrichment of high-field-strength trace elements in granitic rocks. *Contrib. Min. Pet.* **1993**, *114*, 479–488. [CrossRef]
40. Belkasmi, M.; Cuney, M.; Polard, P.J.; Bastoul, A. Chemistry of the Ta-Nb-Sn-W oxide minerals from the Yichun rare metal granite (SE China): Genetic implications and comparison with Maroccan and French Hercynian examples. *Miner. Mag.* **2000**, *64*, 507–533. [CrossRef]
41. Scott, P.W.; Pascoe, R.D.; Hart, F.W. Columbite-tantalite, rutile and other accessory minerals from the St. Austell topaz granite, Cornwall. *Geosci. South-West Engl.* **1998**, *9*, 165–170.
42. Linnen, R.L.; Cuney, M. Granite-Related Rare-Element Deposits and Experimental Constraints on Ta-Nb-W-Sn-Zr-Hf Mineralization. In *Rare-Element Geochemistry and Mineral Deposits*; Linnen, R.L., Samson, I.M., Eds.; *Can. Short Courses Notes*; 2005; Volume 17, pp. 45–67.
43. Linnen, R.L. The solubility of Nb-Ta-Zr-Hf-W in granitic melts with Li and Li + F: Constraints for mineralization in rare-metal granites and pegmatites. *Econ. Geol.* **1998**, *93*, 1013–1025. [CrossRef]
44. Fiege, A.; Kirchner, C.; Barthels, A.; Holtz, F.; Linnen, R.L. Influence of fluorine on the solubility of manganotantalite ($MnTa_2O_6$) and manganocolumbite ($MnNb_2O_6$) in natural rhyolitic, synthetic haplogranitic and pegmatitic melts. *Hall. Jahrb. Geowiss.* **2009**, *31*, 60.